

# Measurement of Single Molecule Conductance: Benzenedithiol and Benzenedimethanethiol

Xiaoyin Xiao, Bingqian Xu, and Nongjian J. Tao\*

*The Center for Solid State Electronics Research, Arizona State University,  
Tempe, Arizona 85287*

*Received November 9, 2003; Revised Manuscript Received December 8, 2003*

## ABSTRACT

We have studied electron transport properties of benzenedithiol and benzenedimethanethiol covalently bonded to gold electrodes by repeatedly creating a large number of molecular junctions. For each molecule, conductance histogram shows peaks at integer multiples of a fundamental conductance value, which is used to identify the conductance of a single molecule. The conductance values of a benzenedithiol and benzenedimethanethiol are  $0.011 G_0$  and  $0.0006 G_0$  ( $G_0 = 2e^2/h$ ), respectively. The conductance peaks are broad, which reflects variations in the microscopic details of different molecular junctions. We have also studied electrochemical gate effect.

Understanding electron transport properties of a molecule electrically wired to two electrodes is an important step toward building a functional device based on single molecules.<sup>1–5</sup> To reliably wire a molecule to electrodes, a widely used strategy is to attach the molecule with two appropriate terminal groups, such as thiols, that can bond covalently to the metal electrodes.<sup>6–13</sup> Two kinds of dithiol molecules have been extensively studied. One is alkanedithiol chains. These molecules are considered highly insulating because of their large energy gap between the HOMO and LUMO, but they are relatively simple and chemically inert, which make them a nice model system to test an experimental technique or theoretical method.<sup>12,14–21</sup> The second dithiol is based on conjugated aryl oligomers, such as oligophenyldithiols and oligophenylene-ethynylenedithiols.<sup>4,11,22–25</sup> The smaller HOMO–LUMO gap and the possibility of functionalizing these molecules make them more attractive for potential molecular electronic applications.

The simplest molecules of the latter group, benzenedithiol (BDT) and benzenedimethanethiol (BDMT), have been investigated experimentally by scanning tunneling microscope (STM)<sup>26,27</sup> and break junction techniques.<sup>6</sup> These pioneering works have stimulated a large theoretical effort to investigate the conductance of these molecules.<sup>28–42</sup> Depending on the models and approximations used by different groups, the theoretical conductance values often differ from the experimental data by several orders of magnitude, which calls for further study of these relatively simple molecules. It has been pointed out that the conductance is sensitive to microscopic details of the molecule–

electrode contact.<sup>5,30,31,34,36,39–44</sup> These details include whether the molecule is properly bonded to both electrodes, what the binding site of the thiol group on the gold electrode is, and how the molecule orients itself with respect to the gold electrode. Due to the difficulty of forming molecular junctions with identical microscopic details, the ability to quickly form and measure a large number of molecular junctions for statistical analysis is important. It has been shown recently that a mechanically controllable break junction can be used to repeatedly form Pt/H<sub>2</sub>/Pt junctions.<sup>13</sup> We have reported an STM break junction approach to create a large number of Au/alkanedithiols/Au junctions.<sup>12</sup> In the present work, we describe the study of electron transport properties of BDT and the closely related BDMT covalently bonded to gold electrodes using this method. Motivated by the possibility of controlling the conductance with a gate electrode,<sup>33,34,36</sup> we have also studied the dependence of the conductance on electrochemical gate voltage.

The technique used to fabricate the molecular junctions and to measure the conductance of the junctions is similar to that described in a previous publication.<sup>12</sup> Briefly, we repeatedly moved a gold STM tip into and out of contact with a gold substrate in the presence of sample molecules on the substrate surface (Figure 1). Because each sample molecule is terminated with two thiol groups, it can bridge the tip and substrate electrodes and form a molecular junction. The process was controlled by a feedback loop that started by driving a gold STM tip into contact with the substrate at a rate of 40 nm/sec. Once the contact was fully established, the feedback loop activated the piezoelectric transducer to pull the STM tip out of the contact. During

\* Corresponding author. E-mail: nongjian.tao@asu.edu

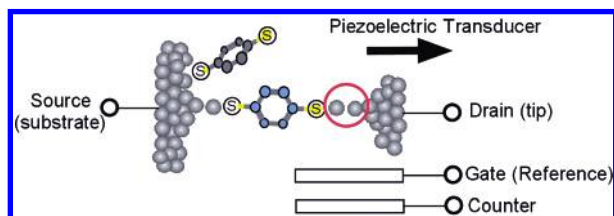


**Figure 1.** Schematic of the experimental setup. A molecular junction is formed by pulling a gold STM tip out of contact with the gold substrate in the presence of sample molecules. The potentials (electrochemical gate voltage) of the gold substrate and gold STM tip were controlled with respect to a reference electrode (Ag wire) using a gold counter electrode and a bipotentiostat.

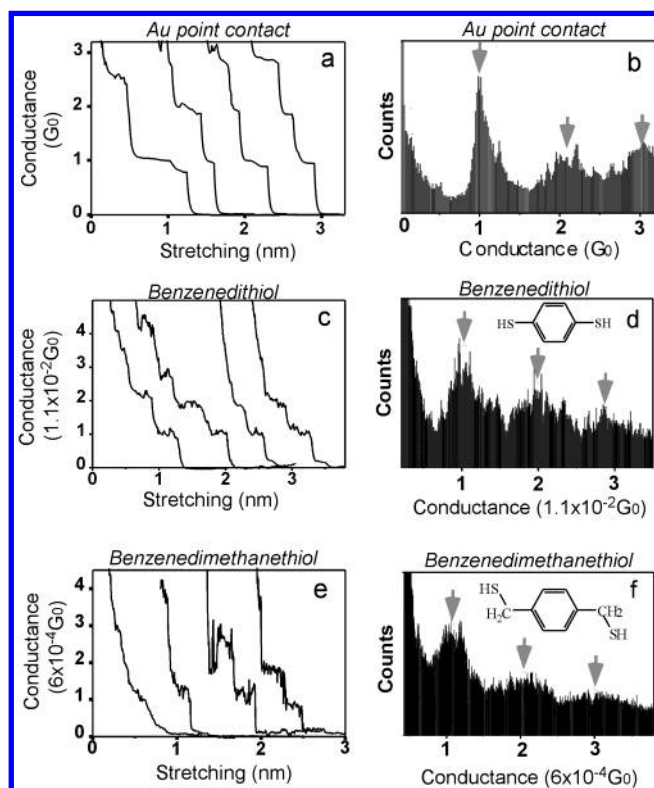


**Figure 2.** Transient conductance trace and the corresponding conductance histogram of gold point quantum contact (a, b) and BDT junctions (c, d) and BDMT junctions (e, f) measured at  $-0.2$  V vs Ag/AgCl in  $0.1$  M  $\text{NaClO}_4$  solutions. The conductance traces were displaced on the  $x$  axis for sake of clarity.

the process, the current flow between the tip and the substrate electrodes was recorded with a fixed bias voltage.

During the initial stage of pulling the tip out of contact with the substrate, the conductance decreased in a stepwise fashion with each step occurring preferentially at an integer multiple of conductance quantum  $G_0 = 2e^2/h$  (Figure 2a). A conductance histogram constructed from one thousand such transient conductance curves reveals pronounced peaks near  $1G_0$ ,  $2G_0$ , and  $3G_0$  (Figure 2b). This well-known conductance quantization occurs when the contact size becomes comparable to the electron Fermi wavelength.<sup>45,46</sup> Since the wavelength for electrons in gold is only a few Å, the appearance of conductance quantization signals the formation of an atomic-scale contact between the tip and the substrate. This conclusion was directly supported by the high-resolution

transmission microscopy images which reveal single-atom contact between two electrodes.<sup>47,48</sup>

When the last gold atom contact is broken by further pulling the tip away, a new sequence of steps in the conductance curves frequently appears in a lower conductance region (Figure 2c–f). Such steps do not appear in every conductance curve. However, the conductance histogram constructed after removing the stepless curves shows conductance peaks centered at  $0.011$ ,  $0.022$ , and  $0.033$   $G_0$  for BDT (Figure 2d). The conductance histogram constructed in a similar way for BDMT exhibits peaks near  $0.0006$ ,  $0.0012$ , and  $0.0018$   $G_0$ , which are 20 times smaller than the corresponding peaks for BDT (Figure 2f). These new peaks are located at much lower values than the conductance peaks of the atomic-scale gold contact. Another important difference is that different molecules have different conductance values. For instance, the conductance (peak position) of *N*-alkanedithiol decreases exponentially with the chain length ( $N$ ).<sup>12</sup> We believe that the conductance steps observed after the breakdown of the gold contact are due to the formation of molecular junctions. The lowest step corresponds to a single molecule bridged between the two gold electrodes.

The conductance from the histogram for a single BDT is  $\sim 0.011$   $G_0$  ( $1.2$  MΩ resistance), significantly greater than the value ( $< 10^{-4}$   $G_0$  near zero bias) determined with a break junction method.<sup>6</sup> The conductance for a BDMT molecule is  $\sim 0.0006$   $G_0$  ( $\sim 21$  MΩ), which is similar to the values extracted from the Coulomb blockade measurement.<sup>26,27</sup> The conductance of BDT is in good agreement with the calculation by Di Ventra et al. who treated the electrodes with a jellium model.<sup>34</sup> However, comparing the measured conductance values with many other theories is less straightforward because most calculated values depend on the binding site of S (or  $\text{SH}^{41}$ ) on gold, and the orientation of the molecule with respect to the electrodes. The distance over which a molecular junction can be stretched for both BDT and BDMT is between  $0.3$  and  $0.6$  nm. This distance is not how long the molecules are stretched. Instead it is due to the stretching of the gold contacts. When a gold atom at the molecule–gold contact is pulled out of the electrode, a nearby surface gold atom moves behind the first atom (marked by red circles in Figure 1). Further pulling can cause a third atom to move behind the second one and form a linear atomic chain. We point out that a similar situation has been observed when separating two gold electrodes from contact, where a chain of gold atoms can be elongated over  $2$  nm.<sup>47,49</sup> This indicates that the S atoms are more likely bonded to the top sites than the hollow or bridge sites of the electrodes. We may further expect that the benzene rings of the molecules align along the stretching direction.

In comparison to previously studied *N*-alkanedithiol and 4,4'-bipyridine, BDT and BDMT are different in two ways. First, only a fraction (30–40%) of the all transient conductance curves has steps and the rest are smooth curves that follow exponential decay. This indicates that the formation of benzenedithiol junctions has a lower probability. This is most likely due to the absence of BDT and BDMT in the solution cell during the formation of individual molecular

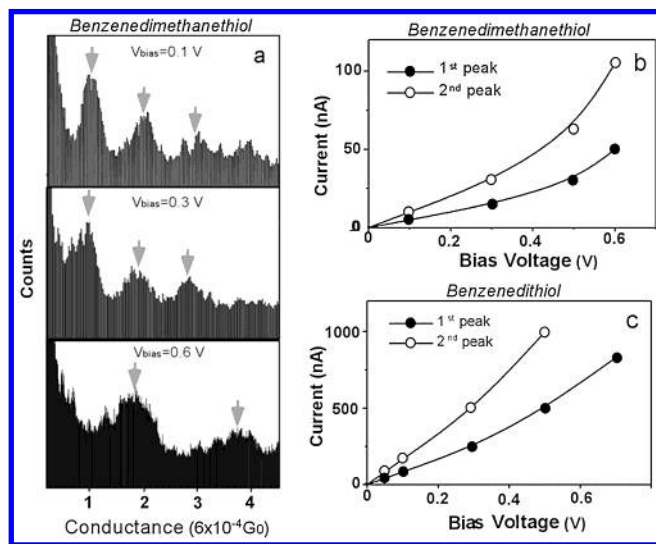


**Figure 3.** (a) Conductance histograms of BDMT at different bias voltages. (b and c)  $I$ - $V$  characteristics of BDT and BDMT molecular junctions. Measurements were done in toluene solutions containing 0.3 mM of the sample molecules.

junctions. Second, the peaks in the conductance histograms of benzenedithiols are much broader than those of alkanedithiols. As we have mentioned above, recent theoretical works<sup>31,32,34,36,39,41</sup> have shown that the conductance of BDT depends not only on the adsorption sites of gold electrodes but also on the molecular orientation in the gold-molecule-gold structure. The broad conductance peaks in the histograms may reflect the variations in the molecule-electrode contact geometry.

We have performed the measurement at various bias voltages. At each voltage, we have obtained a conductance histogram from 300 to 400 transient curves. Figure 3a shows several conductance histograms of BDMT at different bias voltages. The first peak is near 0.0006  $G_0$  and remains constant when the bias voltage is below 0.3 V, which reflects a linear dependence of the current ( $I$ ) on the bias ( $V$ ). However, on increasing the bias voltage to above 0.5 V, the conductance peak shifts toward higher values. The increase in the conductance at large bias voltages is due to nonlinear dependence of  $I$  on  $V$ . At negative bias, the dependence of  $I$  on  $V$  is nearly identical, due to symmetry of the molecular junction. Since,  $I = GV$ , where  $G$  is the conductance values of the histogram peaks, we have obtained the  $I$ - $V$  curves for the first two peaks (Figure 3b). After dividing the  $I$ - $V$  curves of the second peak by 2, the two curves collapse into a single one. We have obtained the  $I$ - $V$  characteristic curve for BDT in a similar way (Figure 3c). The overall shape is similar to that of BDMT, but the nonlinear dependence of  $I$  on  $V$  occurs at a somewhat lower bias voltage. When increasing the voltage to  $\sim 1$  V, the noise level in the current increases rapidly. One possible reason for the increased noise is electrochemical reactions taking place on the tip and the substrate electrodes. Di Ventura et al.<sup>50</sup> reported a dramatic increase in local heating of a single molecule junction when the bias voltage is increased above a certain threshold based on first-principle calculations, which provides another possible explanation of the increased noise at high bias voltages.

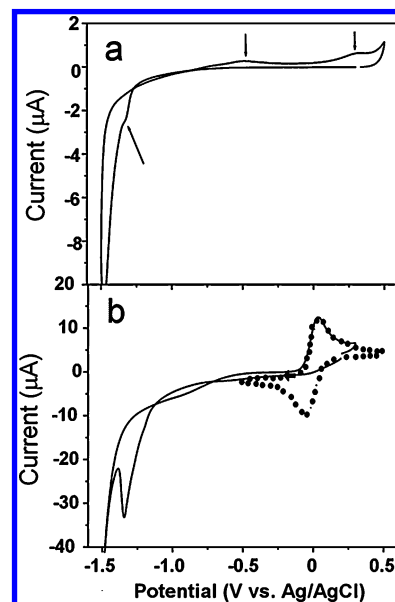


**Figure 4.** Cyclic voltammograms of BDT self-assembled monolayer on gold electrodes in (a) 0.1 M NaClO<sub>4</sub> and (b) 1 mM K<sub>4</sub>Fe(CN)<sub>6</sub> + 0.1 M NaClO<sub>4</sub> solution. The potential sweep rate was 100 mV/s.

The ability to control the electron flow through a molecule between two electrodes with a third electrode is highly desired for molecular electronic devices. For a conventional field effect transistor (FET), a gate electrode is used to control the current flow between a source electrode and a drain electrode. Recent theories have predicted an interesting dependence of the benzenedithiol conductance on gate voltage.<sup>33,34,36</sup> However, to observe the gate effect, a gate field on the order of  $\sim 10$  V/nm is required, which is difficult to reach experimentally. For instance, a typical solid device consists of two electrodes (source and drain electrodes) on top of an oxide gate layer, the actual gate voltage on the molecule is  $\sim (L/t)$  times of the applied gate voltage, where  $L$  is the length of the molecule, which is rather small ( $< 1$  nm) compared to the oxide thickness ( $t > \text{many nm}$ ). In the present work, we used an electrochemical gate applied between the STM tip, or the substrate and a reference electrode in an electrolyte. A much higher gate field can be achieved because the applied voltage falls across the double layer that is only  $\sim 0.5$  nm thick (the diameter of a hydrated ion). This field is close to the gate field required to significantly change the current through a molecule, according to the first-principle calculations by Di Ventura et al.<sup>33,51</sup>

We have established the window within which the electrochemical gate voltage can be varied without electrochemical reactions by measuring the reaction current vs the gate voltage. Figure 4a shows that BDT molecules are stable on the surface when the electrode potential was swept from 0.4 to  $-1.1$  V. The reductive desorption of BDT molecules gives rise to a peak at  $-1.3$  V, which overlaps with hydrogen evolution (i.e., reduction of hydrogen ions to form hydrogen gas). When sweeping the potential anodically, a small peak near  $-0.5$  V, due to readsorption of BDT on the electrode, appears. At  $+0.3$  V, another peak appears, corresponding to oxidative desorption of BDT molecules. Further increasing



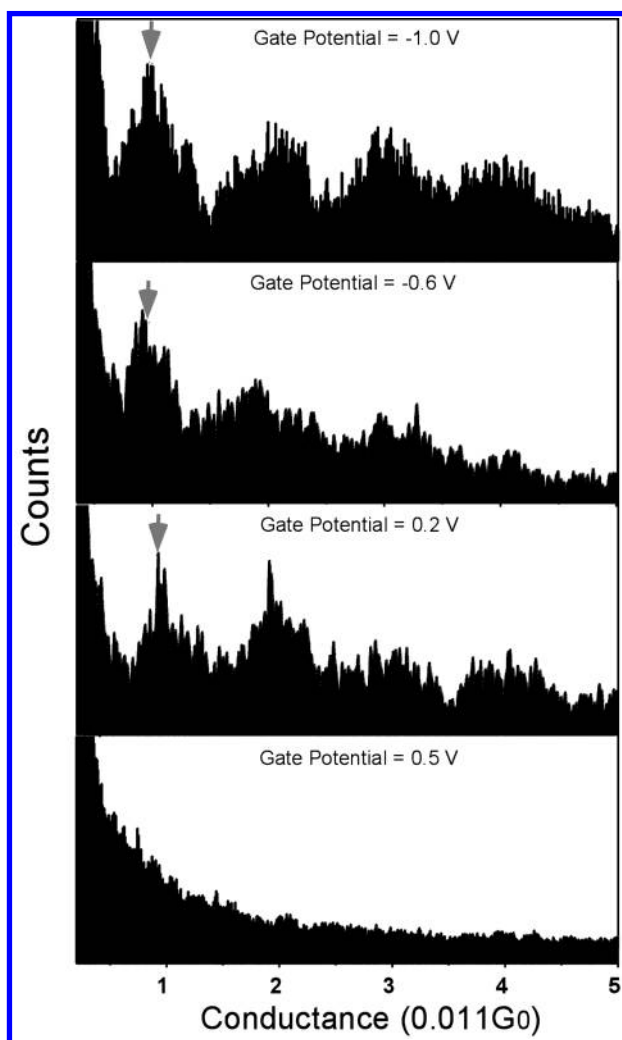


**Figure 5.** Conductance of BDT junctions at different electrochemical gate voltages (electrode potentials) with a fixed bias voltage (100 mV). The measurement was carried out using a gold substrate covered with a self-assembled BDT monolayer and in 0.1 M NaClO<sub>4</sub> solution.

the potential to  $\sim 0.5$  V, oxidation of gold surface takes place. The desorption of BDT molecules in both cathodic and anodic directions was monitored by using Fe(CN)<sub>6</sub><sup>4-</sup> as a probe. In the potential range between  $-1.1$  and  $+0.4$  V, the redox peaks of Fe(CN)<sub>6</sub><sup>4-</sup> are minimal, which indicates that BDT and BDMT molecules form rather dense monolayers and prevent Fe(CN)<sub>6</sub><sup>4-</sup> from reaching the electrode surface. Outside the potential window, the redox peaks increase dramatically, which signals substantial desorption of BDT and BMDT (Figure 4b).

We have varied the gate voltage within the available potential window. The peaks in the conductance histograms are pronounced; however, within the experimental uncertainty, the conductance of the molecules does not depend on the electrochemical gate voltage (Figure 5). Outside of the voltage window, the peaks in the conductance histograms disappear, due to desorption of the molecules from the electrodes. The lack of gate effect is not yet understood, but we speculate the following mechanism as a possible reason. The benzenedithiol molecules are about 0.8 nm long, which defines the separation between the two gold electrodes. The

double layer thickness for each electrode is about 0.5 nm, so there is an overlap between the double layers of the two electrodes, which may affect the actual gate voltage on the molecule.

**Experimental Details.** The gold substrate was prepared by thermally evaporating 100 nm gold on mica in a UHV chamber. Before each experiment, the substrate was briefly annealed in a hydrogen flame and immediately immersed in 1 mM BDT and BDMT ethanol solution for 3–6 min. It was then thoroughly rinsed with ethanol and placed in a Teflon sample cell. The cell was cleaned by boiling it in piranha solution (98% H<sub>2</sub>SO<sub>4</sub>/30% H<sub>2</sub>O<sub>2</sub> = 3:1, v/v), and then sonicating in 18 MΩ·cm water three times (Nanopure system fed with campus distilled water). (Caution: piranha solution reacts violently with most organic materials and must be handled with extreme care.) The STM tip was prepared by cutting a 0.25 mm gold wire (99.999%) with a pair scissors, which was then coated with Apiezon wax in order to reduce ionic conduction and polarization currents. The leakage current due to ionic conduction and polarization was on the order of pA. For electrochemical gate experiment, the potentials of the tip and the substrate were controlled with respect to a quasi reference electrode (Ag wire) using a gold counter electrode and a bipotentiostat (PicoStat, Molecular Imaging Co.). The quasi reference electrode was calibrated against the more commonly used Ag/AgCl (in 3.5 M KCl) reference electrode. The potentials (electrochemical gate) in this paper are quoted vs Ag/AgCl electrode.

**Acknowledgment.** We thank Di Ventra, Stuart Lindsay, Otto Sankey, David Ferry, Jun Li, Gil Speyer, and R. Vaidyanathan and E. Forzani for helpful discussions, and NSF(CHE-0243423)(Xiao) and DOE(DE-FG03-01ER45943)-(Xu) for financial support.

## References

- (1) Nitzan, A.; Ratner, M. A. *Science* **2003**, *300*, 1384.
- (2) Gimzewski, J. K.; Joachim, C. *Science* **1999**, *283*, 1683.
- (3) Joachim, C.; Gimzewski, J. K.; Aviram, A. *Nature* **2000**, *408*, 541.
- (4) Bumm, L. A.; Arnold, J. J.; Cygan, M. T.; Dunbar, T. D.; Burgin, T. P.; Jones, L.; Allara, D. L.; Tour, J. M.; Weiss, P. S. *Science* **1996**, *271*, 1705.
- (5) Nazin, G. V.; Qiu, X. H.; Ho, W. *Science* **2003**, *302*, 77.
- (6) Reed, M. A.; Zhou, C.; Muller, C. J.; Burgin, T. P.; Tour, J. M. *Science* **1997**, *278*, 252.
- (7) Park, J.; Pasupathy, A. N.; Goldsmith, J. L.; Chang, C.; Yaish, Y.; Petta, J. R.; Rinkoski, M.; Sethna, J. P.; Abruna, H. D.; McEuen, P. L.; Ralph, D. C. *Nature* **2002**, *417*, 722.
- (8) Liang, W. J.; Shores, M.; Bockrath, M.; Long, J. R.; Park, H. *Nature* **2002**, *417*, 725.
- (9) Reichert, J.; Ochs, R.; Beckmann, D.; Weber, H. B.; Mayor, M.; Löhneysen, H. v. *Phys. Rev. Lett.* **2002**, *88*, 176804.
- (10) Cui, X. D.; Primak, A.; Zarate, X.; Tomfohr, J.; Sankey, O. F.; Moore, A. L.; Moore, T. A.; Gust, D.; Harris, G.; Lindsay, S. M. *Science* **2001**, *294*, 571.
- (11) Kushmerick, J. G.; Holt, D. B.; Pollack, S. K.; Ratner, M. A.; Yang, J. C.; Schull, T. L.; Naciri, J.; Moore, M. H.; Shashidhar, R. *J. Am. Chem. Soc.* **2002**, *124*, 10654.
- (12) Xu, B. Q.; Tao, N. J. *Science* **2003**, *301*, 1221.
- (13) Smit, R. H. M.; Noat, Y.; Untiedt, C.; Lang, N. D.; van Hemert, M. C.; van Ruitenbeek, J. M. *Nature* **2002**, *419*, 906.
- (14) Cui, X. D.; Primak, A.; Zarate, X.; Tomfohr, J.; Sankey, O. F.; Moore, A. L.; Moore, T. A.; Gust, D.; Nagahara, L. A.; Lindsay, S. M. *J. Phys. Chem. B* **2002**, *106*, 8609.
- (15) Segal, D.; Nitzan, A.; Ratner, M. A.; Davis, W. B. *J. Phys. Chem. B* **2000**, *104*, 2790.

- (16) Tomfohr, J. K.; Sankey, O. F. *Phys. Rev. B* **2002**, *65*, 245105/1.
- (17) Wold, D. J.; Frisbie, C. D. *J. Am. Chem. Soc.* **2000**, *122*, 2970.
- (18) Wold, D. J.; Frisbie, C. D. *J. Am. Chem. Soc.* **2001**, *123*, 5549.
- (19) Slowinski, K.; Fong, H. K. Y.; Majda, M. *J. Am. Chem. Soc.* **1999**, *121*, 7257.
- (20) Slowinski, K.; Majda, M. *J. Electroanal. Chem.* **2000**, *491*, 139.
- (21) York, R. L.; Nguyen, P. T.; Slowinski, K. *J. Am. Chem. Soc.* **2003**, *125*, 5948.
- (22) Hong, S.; Reifengerger, R.; Tian, W.; Datta, S.; Henderson, J.; Kubiak, C. P. *Superlattices and Microstructures* **2000**, *28*, 289.
- (23) Donhauser, Z. J.; Mantooh, B. A.; Kelly, K. F.; Bumm, L. A.; Monnell, J. D.; Stapleton, J. J.; Price, D. W., Jr.; Rawlett, A. M.; Allara, D. L.; Tour, J. M.; Weiss, P. S. *Science* **2001**, *292*, 2303.
- (24) Magoga, M.; Joachim, C. *Phys. Rev. B* **1997**, *56*, 4722.
- (25) Lee, J.-O.; Lientschnig, G.; Wiertz, F.; Struijk, M.; Janssen, R. A. J.; Egberink, R.; Reinhoudt, D. N.; Hadley, P.; Dekker, C. *Nano Lett.* **2003**, *3*, 113.
- (26) Dorogi, M.; Gomez, J.; Osifchin, R.; Andres, R. P.; Reifengerger, R. *Phys. Rev. B* **1995**, *52*, 9071.
- (27) Andres, R. P.; Bein, T.; Dorogi, M.; Feng, S.; Henderson, J. I.; Kubiak, C. P.; Mahoney, W.; Osifchin, R. G.; Reifengerger, R. *Science* **1996**, *272*, 1323.
- (28) Samanta, M. P.; Tian, W.; Datta, S.; Henderson, J. I.; Kubiak, C. P. *Phys. Rev. B* **1996**, *53*, R7626.
- (29) Datta, S.; Tian, W. D.; Hong, S. H.; Reifengerger, R.; Henderson, J. I.; Kubiak, C. P. *Phys. Rev. Lett.* **1997**, *79*, 2530.
- (30) Emberly, E. G.; Kirczenow, G. *Phys. Rev. B* **1998**, *58*, 10911.
- (31) Yaliraki, S. N.; Kemp, M.; Ratner, M. A. *J. Am. Chem. Soc.* **1999**, *121*, 3428.
- (32) Yaliraki, S. N.; Roitberg, A. E.; Gonzalez, C.; Mujica, V.; Ratner, M. A. *J. Chem. Phys.* **1999**, *111*, 6997.
- (33) Di Ventra, M.; Pantelides, S. T.; Lang, N. D. *Appl. Phys. Lett.* **2000**, *76*, 3448.
- (34) Di Ventra, M.; Kim, S. G.; Pantelides, S. T.; Lang, N. D. *Phys. Rev. Lett.* **2001**, *86*, 288.
- (35) Kornilovitch, P. E.; Bratkovsky, A. M. *Phys. Rev. B* **2001**, *64*, 195413/1.
- (36) Bratkovsky, A. M.; Kornilovitch, P. E. *Phys. Rev. B* **2003**, *67*, 115307/1.
- (37) Wang, C.-K.; Luo, Y. *J. Chem. Phys.* **2003**, *119*, 4923.
- (38) Wang, C.-K.; Fu, Y.; Luo, Y. *Phys. Chem. Chem. Phys.* **2001**, *3*, 5017.
- (39) Nara, J.; Kino, H.; Kobayashi, N.; Tsukada, M.; Ohno, T. *Thin Solid Films* **2003**, *438–439*, 221.
- (40) Tikhonov, A.; Coalson, R. D.; Dahnovsky, Y. *J. Chem. Phys.* **2002**, *117*, 567.
- (41) Stokbro, K.; Taylor, J.; Brandbyge, M.; Mozos, J.-L.; Ordejon, P. *Comput. Mater. Sci.* **2003**, *27*, 151.
- (42) Tomfohr, J. K. Ph.D. Thesis, 2003, Arizona State University.
- (43) Moresco, F.; Gross, L.; Alemani, M.; Rieder, K. H.; Tang, H.; Gourdon, A.; Joachim, C. *Phys. Rev. Lett.* **2003**, *91*, 036601/1.
- (44) Emberly, E. G.; Kirczenow, G. *Phys. Rev. B* **2001**, *64*, 235412/1.
- (45) Pascual, J. I.; Mendez, J.; Gomez-Herrero, J.; Baro, A. M.; Garcia, N.; Binh, V. T. *Phys. Rev. Lett.* **1993**, *71*, 1852.
- (46) Krans, J. M.; Ruitenbeek, J. M. v.; Fisun, V. V.; Yanson, I. K.; Jongh, L. J. D. *Nature* **1995**, *375*, 767.
- (47) Ohnishi, H.; Kondo, Y.; Takayanagi, K. *Nature* **1998**, *395*, 780.
- (48) Rodrigues, V.; Fuhrer, T.; Ugarte, D. *Phys. Rev. Lett.* **2000**, *85*, 4124.
- (49) Yanson, A. I.; Rubio Bollinger, G.; van den Brom, H. E.; Agrait, N.; van Ruitenbeek, J. M. *Nature* **1998**, *395*, 783.
- (50) Chen, Y.-C.; Zwolak, M.; Di Ventra, M. *Nano Lett.* **2003**, *3*, 1691.
- (51) Di Ventra, M.; Lang, N. D.; Pantelides, S. T. *Chem. Phys.* **2002**, *281*, 189.

NL035000M